Cell Reports, Volume *39*

Supplemental information

Unravelling the sex-specific diversity and functions of adrenal gland macrophages

Bastien Dolfi, Alexandre Gallerand, Maria M. Firulyova, Yingzheng Xu, Johanna Merlin, Adélie Dumont, Alexia Castiglione, Nathalie Vaillant, Sandrine Quemener, Heidi Gerke, Marion I. Stunault, Patricia R. Schrank, Seung-Hyeon Kim, Alisha Zhu, Jie Ding, Jerome Gilleron, Virginie Magnone, Pascal Barbry, David Dombrowicz, Christophe Duranton, Abdelilah Wakkach, Claudine Blin-Wakkach, Burkhard Becher, Sophie Pagnotta, Rafael J. Argüello, Pia Rantakari, Svetoslav Chakarov, Florent Ginhoux, Konstantin Zaitsev, Ki-Wook Kim, Laurent Yvan-Charvet, Rodolphe R. Guinamard, Jesse W. Williams, and Stoyan Ivanov

Sup. Table 1

gene	p_val	avg_logFC (female over male)	pct.1	pct.2	p_val_adj
Xist	0	1.54951258733711	0.828	0	0
Rpl35	7.62774369759271e-40	0.332795131151709	0.975	0.916	1.1416443992187e-35
Apoc2	3.69158130258448e-26	0.332692544859788	0.379	0.167	5.52518973557819e-22
AA467197	6.22673290146039e-23	0.369648525877762	0.16	0.037	9.31955113361576e-19
Lyz2	2.17567047442043e-22	0.386902156024932	0.999	0.999	3.25632599906506e-18
Tsc22d3	6.49050153643698e-22	0.329842436397367	0.611	0.429	9.71433364958522e-18
Fxyd5	8.32816037140203e-22	0.27680960279782	0.944	0.892	1.24647576278774e-17
Ap1s2	1.73034399696515e-21	0.294384138791506	0.516	0.367	2.58980586025774e-17
Sla	3.91862476256913e-20	0.266959924479275	0.497	0.332	5.86500568213722e-16
Ly6a	1.0545988034916e-15	0.366701350118315	0.206	0.097	1.57841802918587e-11
Cebpb	8.00698976030681e-15	0.250943124974004	0.712	0.549	1.19840615742512e-10
Msrb1	5.40275053801241e-14	0.275219903461956	0.558	0.398	8.08629673024318e-10
Tmsb10	4.60848480745743e-12	0.380808925495099	0.801	0.725	6.89751921132154e-08
Ms4a4c	8.66898423345473e-11	0.25134064025716	0.4	0.286	1.29748687022117e-06
Chil3	4.8237747978503e-10	0.394563532638321	0.186	0.087	7.21974373994254e-06
Ifitm3	3.73254227181447e-08	0.266876571843615	0.88	0.835	0.000558649601822472
Ly6c2	3.5363257330096e-07	0.29637517528339	0.18	0.097	0.00529281872459546
Plac8	4.98692265535371e-07	0.460921076326878	0.294	0.193	0.0074639271382679
Apoe	7.50291402455461e-07	0.48830922785863	0.969	0.955	0.0112296114205509
S100a6	1.08763499763158e-06	0.276562829675311	0.591	0.514	0.0162786330095518

Table S1.
List of genes differentially expressed among myeloid cells in female and male mice. This table is related to figure 2.

Sup. Fig. 1

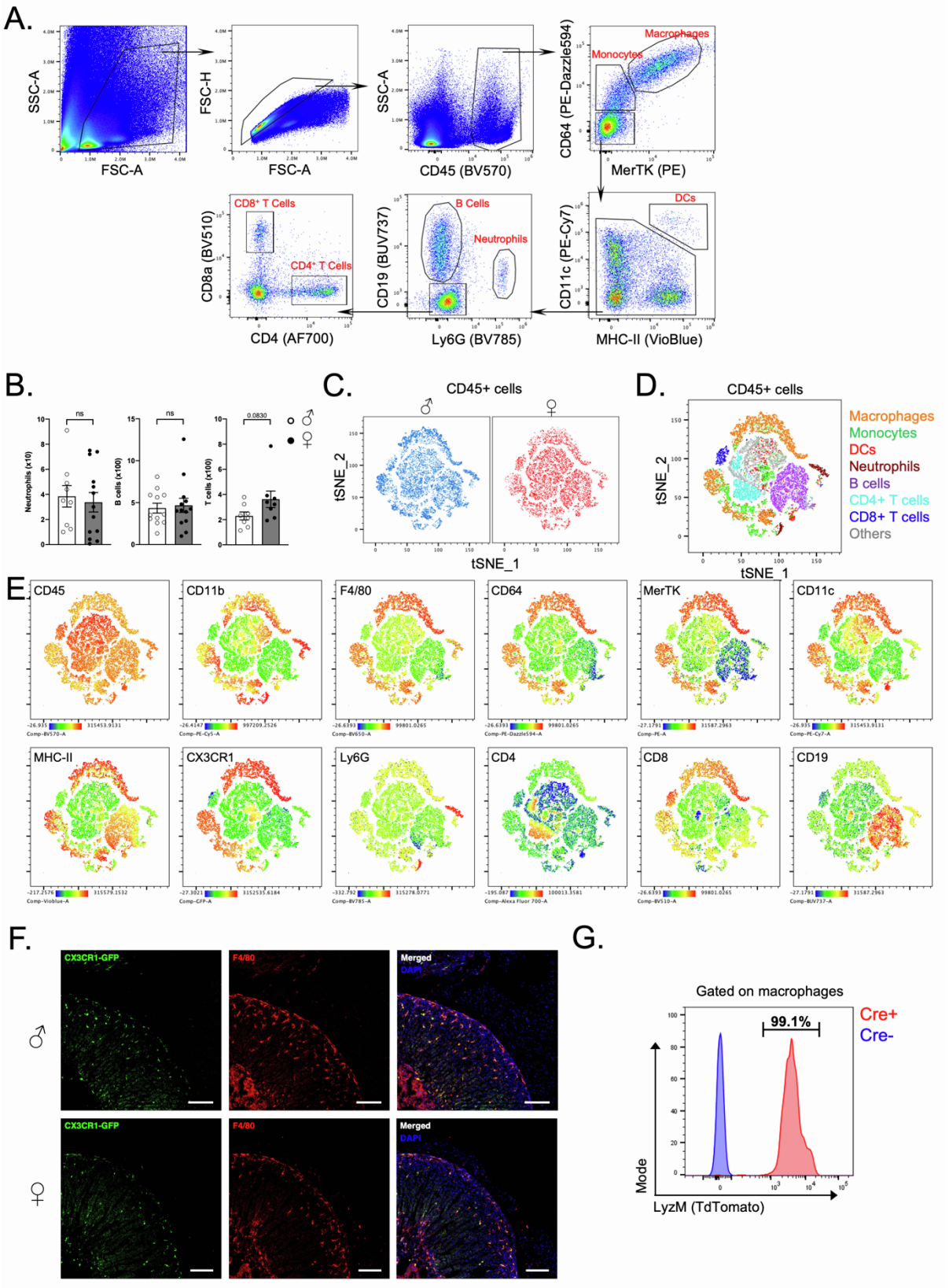
A.
SSC-A
FSC-A
FSC-H
FSC-A
SSC-A
CD45 (BV570)
CD64 (PE-Dazzle594)
MerTK (PE)
Macrophages
Monocytes
CD8a (BV510)
CD4 (AF700)
CD8+ T Cells
CD4+ T Cells
CD19 (BUV737)
Ly6G (BV785)
B Cells
Neutrophils
CD11c (PE-Cy7)
MHC-II (VioBlue)
DCs
B.
Neutrophils (x10)
B cells (x100)
T cells (x100)
ns
ns
0.0830
C.
CD45+ cells
tSNE_2
tSNE_1
D.
CD45+ cells
tSNE_2
tSNE_1
Macrophages
Monocytes
DCs
Neutrophils
B cells
CD4+ T cells
CD8+ T cells
Others
E.
CD45
CD11b
F4/80
CD64
MerTK
CD11c
MHC-II
CX3CR1
Ly6G
CD4
CD8
CD19
F.
CX3CR1-GFP
F4/80
Merged
DAPI
G.
Gated on macrophages
99.1%
Cre+
Cre-
Mode
LyzM (TdTomato)

Figure S1. Flow cytometry analysis of immune cell diversity in male and female adrenal glands. This figure in complementary to figure 1.

(**A**) Gating strategy used to identify adrenal gland immune cells. Concatenated data from 8 7-week-old female mice. (**B**) Quantification of neutrophils (♂ n=9 and ♀ n=13), B cells (♂ n=12 and ♀ n=13) and T cells (♂ n=8 and ♀ n=8) in male and female adrenal glands. Data pooled from one (T cells) or two (neutrophils and B cells) independent experiments. (**C**) Clustering of $CD45^+$ adrenal gland cells from male and female $CX3CR1^{GFP}$ mice using unsupervised t-distributed stochastic neighbor embedding (tSNE) analysis of flow cytometry data. Panel : CD40 (BUV395) ; CD24 (BUV496) ; CD80 (BUV615) ; CD19 (BUV737) ; F4/80 (BV650) ; Ly6G (BV785) ; CX3CR1 (GFP reporter) ; MerTK (PE) ; CD64 (PE-Dazzle594) ; CD11b (PE-Cy5) ; CD206 (PerCP-Cy5.5) ; Timd4 (PerCP-eFluor710) ; CD11c (PE-Cy7) ; Lyve1 (eFluor660) ; CD4 (AF700) ; CCR2 (APC-Fire750). (**D**) Identification of adrenal gland immune subsets. Cells were gated manually and overlaid on tSNE plot to identify clusters. Macrophages : $CD45^+$ $CD64^+$ $MerTK^+$. Monocytes : $CD45^+$ $MerTK^-$ $CD11b^+$ $CX3CR1^+$. Dendritic Cells (DCs) : $CD45^+$ $MerTK^-$ $CD11c^+$ $MHC\text{-}II^+$. Neutrophils : $CD45^+$ $CD11b^+$ $Ly6G^+$. B cells : $CD45^+$ $MerTK^-$ $CD11c^-$ $MHC\text{-}II^+$ $CD19^+$. CD4+ T cells : $CD45^+$ $MerTK^-$ $MHC\text{-}II^-$ $CD4^+$. CD8+ T cells : $CD45^+$ $MerTK^-$ $MHC\text{-}II^-$ $CD8^+$. (**E**) tSNE representation of the expression levels of CD45, CD11b, F4/80, CD64, MerTK, CD11c, MHC-II, CX3CR1, Ly6G, CD4, CD8 and CD19 among adrenal gland $CD45^+$ cells. (**F**) Microscopy analysis of F4/80 staining in adrenal glands of $CX3CR1^{GFP/+}$ mice. Scale bar : 100μm. (**G**) Flow cytometry analysis of TdTomato expression in adrenal gland macrophages from 8-week-old male $Lyz2^{cre}$ x $R26^{TdTomato}$ mice. Data from one experiment. All data are represented in means ± SEM. Statistical analysis was performed using two-tailed Mann-Whitney tests. ns $p>0.05$; * $p<0.05$; ** $p<0.01$; *** $p<0.001$; **** $p<0.0001$.

Sup. Fig. 2

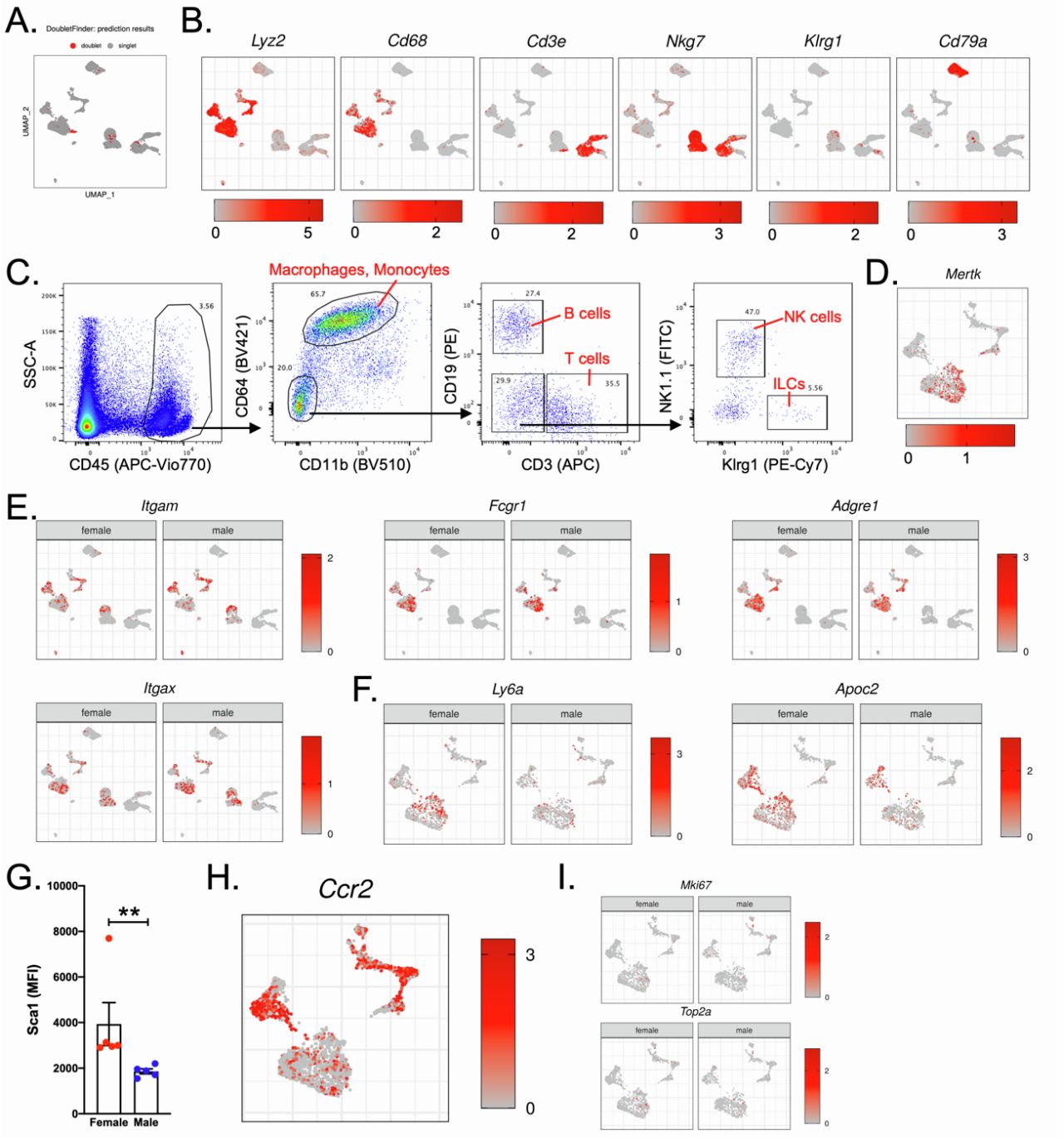
A.
DoubletFinder: prediction results
doublet
singlet
UMAP_2
UMAP_1
B.
Lyz2
Cd68
Cd3e
Nkg7
Klrg1
Cd79a
C.
Macrophages, Monocytes
B cells
T cells
NK cells
ILCs
SSC-A
CD45 (APC-Vio770)
CD64 (BV421)
CD11b (BV510)
CD19 (PE)
CD3 (APC)
NK1.1 (FITC)
Klrg1 (PE-Cy7)
D.
Mertk
E.
Itgam
Fcgr1
Adgre1
Itgax
female
male
F.
Ly6a
Apoc2
G.
Sca1 (MFI)
Female
Male
H.
Ccr2
I.
Mki67
Top2a

Figure S2. Single cell RNA-seq analysis of adrenal gland immune cell diversity. This figure is complementary to figure 2.

(**A**) Identification of doublets in scRNA-seq data using the DoubletFinder package. Doublets were removed from analysis. (**B**) scRNA-seq analysis of genes used to identify cell types (*Lyz2*, *CD68*, *CD3e*, *Nkg7*, *Klrg1* and *CD79a*). (**C**) Flow cytometry plots validating the presence of immune cell types corresponding to clusters identified in the scRNA-seq analysis. (**D**) scRNA-seq analysis of *Mertk* expression among adrenal gland myeloid cells. (**E**) scRNA-seq analysis of myeloid cell canonical markers by adrenal gland $CD45^+$ cells from 7-week-old male and female mice. (**F**) scRNA-seq analysis of sex-enriched genes in adrenal gland myeloid cells. (**G**) Flow cytometry analysis of Sca1 expression in female and male mice (n=5 mice per group). Data pooled from two independent experiments. (**H**) scRNA-seq analysis of *CCR2* expression among adrenal gland myeloid cells. (**I**) scRNA-seq analysis of *Mki67* and *Top2a* mRNA expression. All data are represented in means ± SEM. Statistical analysis was performed using two-tailed Mann-Whitney tests. ns $p>0.05$; * $p<0.05$; ** $p<0.01$; *** $p<0.001$; **** $p<0.0001$.

Sup. Fig. 3

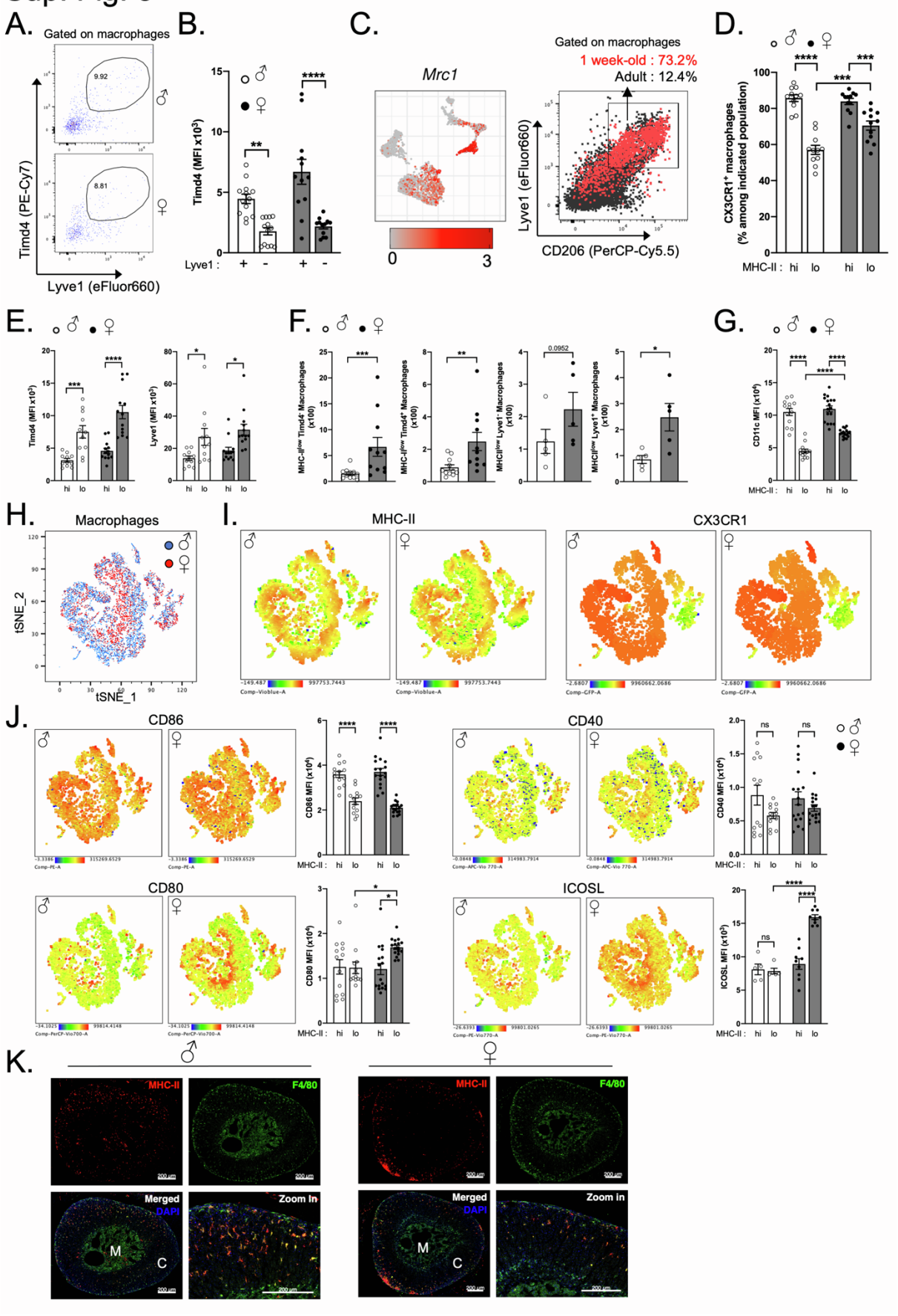
A.
Gated on macrophages
9.92
8.81
Timd4 (PE-Cy7)
Lyve1 (eFluor660)
B.
Timd4 (MFI x10³)
Lyve1 :
C.
Mrc1
0
3
Gated on macrophages
1 week-old : 73.2%
Adult : 12.4%
Lyve1 (eFluor660)
CD206 (PerCP-Cy5.5)
D.
CX3CR1⁺ macrophages (% among indicated population)
MHC-II : hi lo hi lo
E.
Timd4 (MFI x10³)
Lyve1 (MFI x10³)
F.
MHC-II^low Timd4⁺ Macrophages (x100)
MHC-II^low Timd4⁺ Macrophages (x100)
MHCII^low Lyve1⁻ Macrophages (x100)
MHCII^low Lyve1⁺ Macrophages (x100)
0.0952
G.
CD11c MFI (x10⁴)
H.
Macrophages
tSNE_2
tSNE_1
I.
MHC-II
CX3CR1
J.
CD86
CD86 MFI (x10⁴)
CD40
CD40 MFI (x10⁴)
CD80
CD80 MFI (x10⁴)
ICOSL
ICOSL MFI (x10³)
ns
K.
MHC-II
F4/80
Merged
DAPI
Zoom in
M
C
200 µm

Figure S3. MHC-II expression identifies two macrophage populations with sex-specific abundance and distribution. This figure is complementary to figures 3 and 4.

(**A**) Representative plots showing adrenal gland macrophage Timd4 and Lyve1 expression in male and female mice. Data representative of at least 3 independent experiments. (**B**) Mean Timd4 fluorescence intensity among Lyve1^{+} and Lyve1^{-} macrophage subsets in male and female mice. ♂ n=13 and ♀ n=12. Data pooled from 2 independent experiments. (**C**) (Left) scRNA-seq analysis of *Mrc1* mRNA expression and (Right) representative plot showing adrenal gland macrophage Lyve1 and CD206 expression in 1- and 9-week-old male mice. Data from one experiment. (**D**) Proportions of CX3CR1^{+} cells among MHC-II^{high} and MHC-II^{low} adrenal gland macrophages from male and female CX3CR1^{GFP} mice. ♂ n=11 and ♀ n=12. Data pooled from 2 independent experiments. (**E**) Mean Timd4 and Lyve1 fluorescence intensity among MHC-II^{high} and MHC-II^{low} adrenal gland macrophages from male and female mice. ♂ n=12 and ♀ n=13. Data pooled from 2 independent experiments. (**F**) Quantification of MHC-II^{low} adrenal gland macrophage subsets according to Lyve1 and Timd4 expression in 7-week-old male and female mice. Timd4 subsets : ♂ n=11 and ♀ n=11. Data pooled from 2 independent experiments. Lyve1 subsets : ♂ n=5 and ♀ n=5. Data from one experiment. (**G**) Mean CD11c fluorescence intensity among MHC-II^{high} and MHC-II^{low} adrenal gland macrophages from male and female mice. ♂ n=13 and ♀ n=17. Data pooled from 3 independent experiments. (**H**) Clustering of adrenal gland macrophages from male and female CX3CR1^{GFP} mice using unsupervised t-distributed stochastic neighbor embedding (tSNE) analysis of flow cytometry data. Panel : CD24 (BUV496) ; CD19 (BUV737) ; MHC-II (VioBlue) ; CD11b (BV510) ; CD45 (BV570) ; F4/80 (BV650) ; CX3CR1 (GFP reporter) ; CD86 (PE) ; CD64 (PE-Dazzle594) ; CD11c (PE-Cy5) ; CD80 (PerCP-Vio700) ; ICOSL (PE-Vio770) ; Ly6C (APC) ; CD40 (APC-Vio770). Data representative of 3 independent experiments. (**I**) tSNE representation of MHC-II and CX3CR1 expression levels in adrenal gland macrophages from male and female CX3CR1^{GFP} mice. Data representative of 3 independent experiments. (**J**) tSNE representation and quantification of CD86, CD80, CD40 and ICOSL expression levels in adrenal gland macrophages from male and female CX3CR1^{GFP} mice. ♂ n=13 and ♀ n=17. Pooled data from 2 (ICOSL) or 3 (CD86, CD80, CD40) independent experiments. (**K**) Fluorescence microscopy analysis of F4/80 and MHC-II expression in adrenal glands from 7-week-old male and female wild-type mice. Scale bar : 200μm. M (medulla); C (cortex). Data representative of at least 3 independent experiments. All data are represented in means ± SEM. Statistical analysis was performed using two-way ANOVA with Bonferroni's post-test (panels B, D, E, F, G and J) or two-tailed Mann-Whitney tests (panel G). ns $p>0.05$; * $p<0.05$; ** $p<0.01$; *** $p<0.001$; **** $p<0.0001$.

Sup. Fig. 4

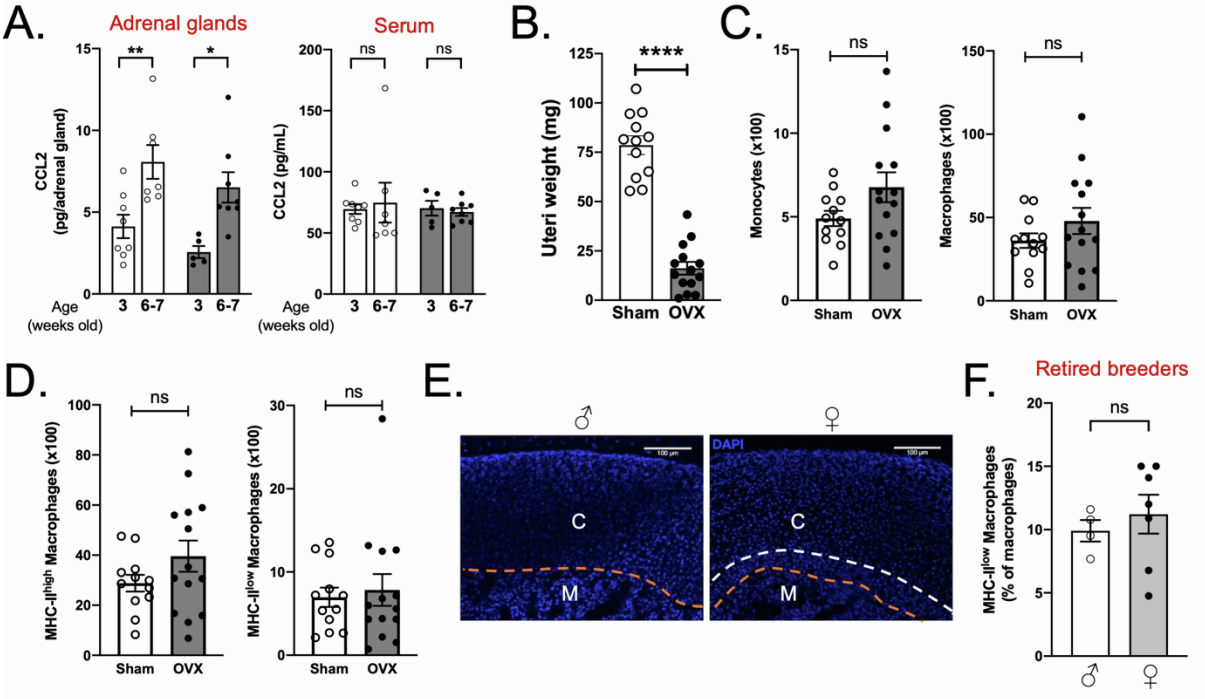

Figure S4. Ovariectomy does not affect adrenal gland macrophage content. This figure is complementary to figure 5.

(**A**) CCL2 levels in adrenal gland homogenates and serum from 3 (♂ n=8 and ♀ n=5) or 6 to 7 (♂ n=7 and ♀ n=8) week-old male and female wild-type mice. Data pooled from 4 independent experiments. (**B**) Weight of uteri from sham-operated (n=12) and OVX (n=14) mice. Data pooled from 2 independent experiments. (**C**) Quantification of adrenal gland monocytes and macrophages in ovariectomized (n=14) and sham-operated (n=12) wild-type mice. Data pooled from 2 independent experiments. (**D**) Quantification of adrenal gland MHC-II^{low} and MHC-II^{high} macrophages in ovariectomized (n=14) and sham-operated (n=12) wild-type mice. Data pooled from 2 independent experiments. (**E**) Confocal microscopy analysis of adrenal glands from male and female 4-week-old wild-type mice. Orange dots indicate the border between the cortex (C) and the medulla (M). The X-Zone is comprised between white and orange dots. Scale bar : 100um. (**F**) Proportions of MHC-II^{low} adrenal gland macrophages in male and female retired breeders (♂ n=4 and ♀ n=7). Data pooled from 2 independent experiments. All data are represented in means ± SEM. Statistical analysis was performed using two-way ANOVA with Bonferroni's post-test (panel A) or two-tailed Mann-Whitney tests (panels B, C, D and F). ns p>0.05 ; * p<0.05 ; ** p<0.01 ; *** p<0.001 ; **** p<0.0001.

Sup. Fig. 5

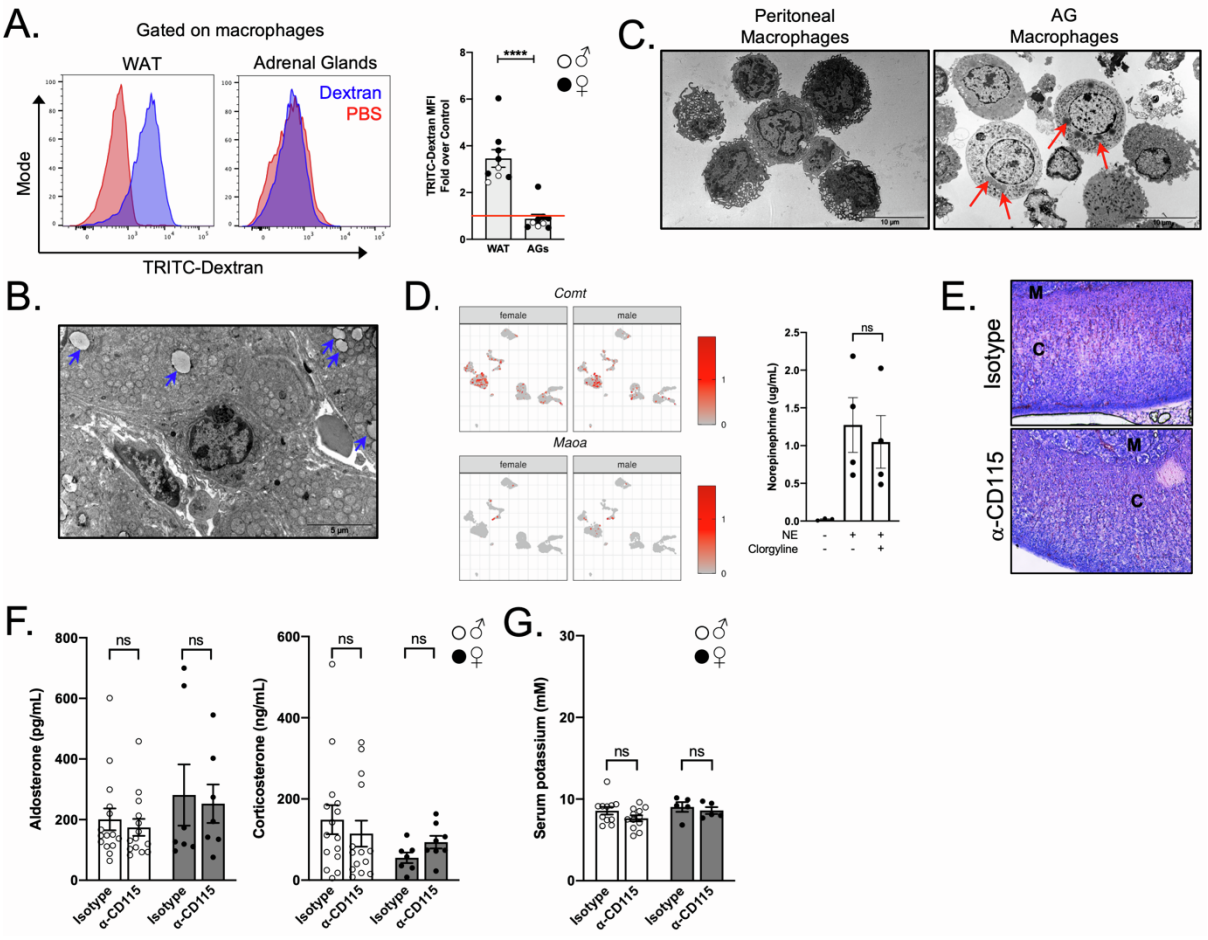
A.
Gated on macrophages
WAT
Adrenal Glands
Dextran
PBS
Mode
TRITC-Dextran
TRITC-Dextran MFI Fold over Control
****
WAT
AGs
B.
C.
Peritoneal Macrophages
AG Macrophages
D.
Comt
Maoa
female
male
Norepinephrine (ug/mL)
ns
NE
Clorgyline
E.
Isotype
α-CD115
M
C
F.
Aldosterone (pg/mL)
Corticosterone (ng/mL)
ns
Isotype
α-CD115
G.
Serum potassium (mM)

Figure S5. Macrophage depletion does not alter adrenal gland architecture and hormone production at steady state. This figure is complementary to figure 6.
(**A**) Representative flow cytometry plots (left) and quantification (right) of TRITC-Dextran uptake by adipose tissue and adrenal gland macrophages 20 minutes after intravenous injection of 1mg 65-85kDa TRITC-Dextran. (♂ n=3 and ♀ n=6). Data from one experiment. (**B**) Electron microscopy analysis of adrenal gland macrophages. Blue arrows indicate the presence of lipid droplets in stroma. Scale bar : 5μm. (**C**) Electron microscopy analysis of purified peritoneal and adrenal gland macrophages. Red arrows indicate the presence of lipid droplets in macrophages. Scale bar : 10μm. Data from one experiment. (**D**) (Left) scRNA-seq analysis of *Maoa* and *Comt* mRNA expression and (Right) norepinephrine levels after overnight culture of cell-sorted adrenal gland macrophages in the presence/absence of norepinephrine and/or clorgyline. n=3 (baseline) or 4 (+NE) biological replicates. Data from 3 pooled experiments. (**E**) Microscopy analysis of adrenal gland morphology in isotype control-treated and α–CD115-treated wild-type mice using H&E staining. Data from one experiment. (**F**) Serum aldosterone and corticosterone levels in isotype control-treated (♂ n=15 and ♀ n=7) and α–CD115-treated (♂ n=14 and ♀ n=7-8) male and female wild-type mice. (**G**) Serum K^+ levels in isotype control-treated (♂ n=11 and ♀ n=5) and α–CD115-treated (♂ n=12 and ♀ n=5) male and female wild-type mice. Pooled data from 3 independent experiments. Statistical analysis was performed using two-way ANOVA with Bonferroni's post-test (panels F and G), one-way ANOVA with Bonferroni's post-test (panel D) or two-tailed Mann-Whitney tests (panel A). ns $p>0.05$; * $p<0.05$; ** $p<0.01$; *** $p<0.001$; **** $p<0.0001$.

Sup. Fig. 6

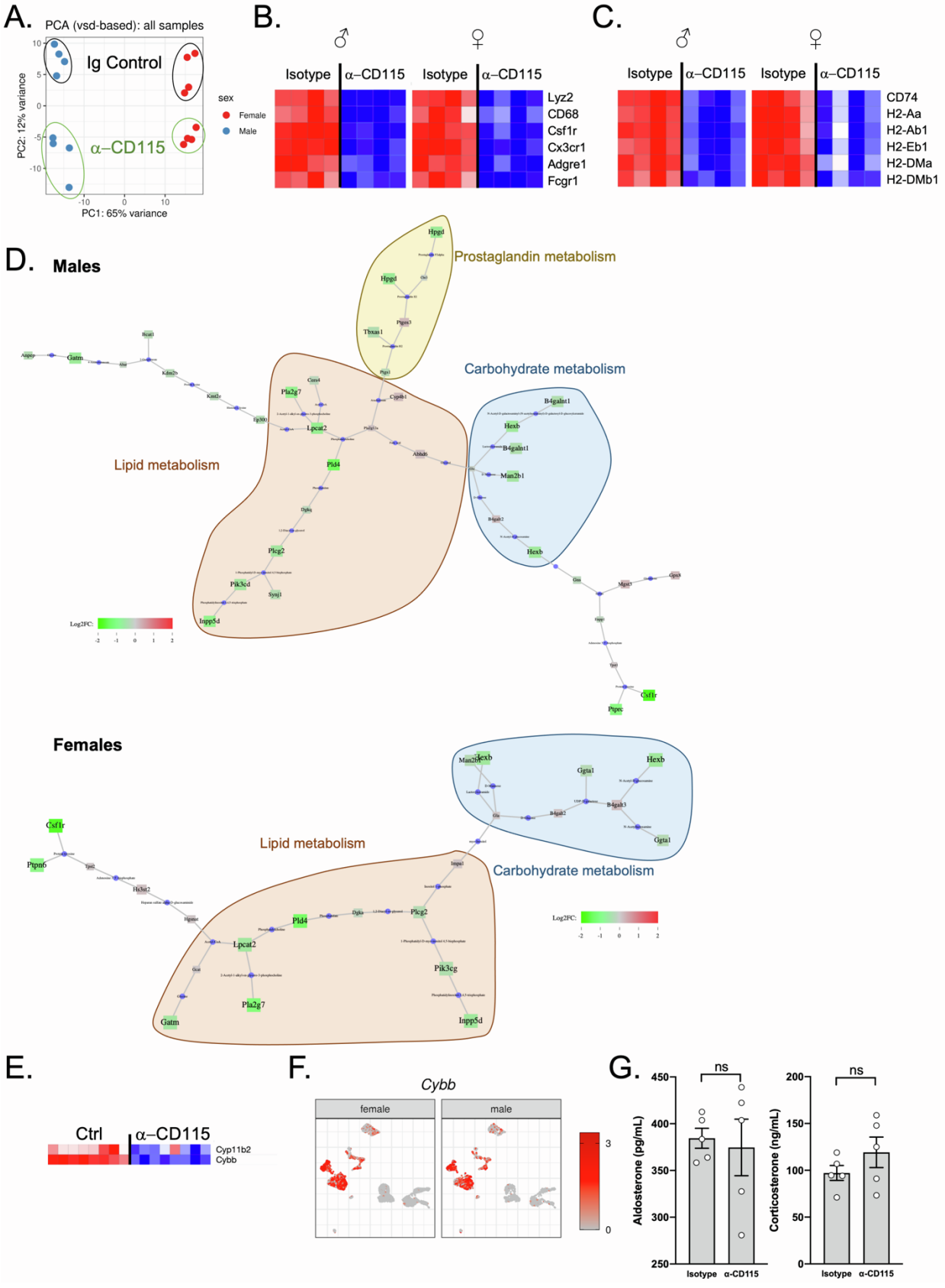
A.
PCA (vsd-based): all samples
Ig Control
α–CD115
PC2: 12% variance
PC1: 65% variance
sex
Female
Male
B.
♂
♀
Isotype
α–CD115
Isotype
α–CD115
Lyz2
CD68
Csf1r
Cx3cr1
Adgre1
Fcgr1
C.
♂
♀
Isotype
α–CD115
Isotype
α–CD115
CD74
H2-Aa
H2-Ab1
H2-Eb1
H2-DMa
H2-DMb1
D.
Males
Prostaglandin metabolism
Carbohydrate metabolism
Lipid metabolism
Females
Lipid metabolism
Carbohydrate metabolism
E.
Ctrl
α–CD115
Cyp11b2
Cybb
F.
Cybb
female
male
3
0
G.
ns
ns
Aldosterone (pg/mL)
Corticosterone (ng/mL)
Isotype
α-CD115
Isotype
α-CD115

Figure S6. Macrophage depletion affects adrenal gland lipid metabolism. This figure is complementary to figure 6.

(**A**) Principal Component Analysis (PCA) of adrenal gland bulk RNA-seq from isotype control-treated and α–CD115-treated male and female wild-type mice. (**B**) RNA-seq analysis of myeloid cell-related genes in adrenal glands from isotype control-treated and α–CD115-treated male and female wild-type mice. (**C**) RNA-seq analysis of MHC-II-related genes in adrenal glands from isotype control-treated and α–CD115-treated male and female wild-type mice. (**D**) Transcriptional analysis of metabolic pathways in adrenal glands from α–CD115 or isotype control treated male and female mice. The size of nodes represent the significance of changes in gene expression : bigger size of nodes means lower p-values. A high resolution version of this panel is supplied as supplementary item 3. (**E**) RNA-seq analysis of *Cyp11b2* and *Cybb* expression in adrenal glands from isotype control-treated and α–CD115-treated wild-type mice. (**F)** scRNA-seq analysis of *Cybb* mRNA expression. (**G**) Serum aldosterone and corticosterone levels in α–CD115 (n=5) or isotype control-treated (n=5) female wild-type mice submitted to a 12-hour cold challenge. Data from one experiment. Statistical analysis was performed using two-tailed Mann-Whitney tests (panel G). ns $p>0.05$.